In Vitro Dynamic Dialysis Technique to Determine Solute–Protein Binding Interactions

PETER C. FARRELL, ROBERT P. POPOVICH, and ALBERT L. BABB

Abstract □ A novel technique to evaluate solute–protein binding characteristics is presented with some preliminary data. The technique is based upon a dual closed-loop dialysis system using radioactive tracers. The method permits easy determination of binding interactions and membrane permeabilities at a series of temperatures and, thereby, readily enables evaluation of enthalpy and entropy effects of binding interactions. At present, the technique is being used to study protein interactions of various waste metabolites, drugs, and essential amino acids and hormones.

Keyphrases □ Solute–protein binding—determination, *in vitro* dialysis □ Protein–solute binding—determination, *in vitro* dialysis □ Dialysis, closed loop—solute–protein binding levels, hemodialysis removal rates □ Hemodialysis removal rates—dynamic closed-loop dialysis

Present techniques to determine solute–protein interactions can be divided into three categories: (*a*) direct visualization of the solute–protein complex, (*b*) electrostatic methods, and (*c*) indirect or substractive methods.

A complete review of the more common analytical procedures comprising these categories is provided by Steinhardt and Reynolds (1). Each technique has limitations; the choice of method, to a large extent, depends upon the system to be investigated.

For both direct methods and electrostatic procedures, there can be problems in distinguishing solute–protein interactions from system noise. These difficulties can be caused by a number of factors but are caused primarily by equipment sensitivity and solvent artifacts.

The subtractive methods are also plagued with certain artifacts. For example, methods such as equilibrium dialysis, which employ semipermeable membranes, have the inherent complications of osmotic and Donnan effects. Probably the major problem with indirect observations of binding is that if the binding is small, there is an inherently large error, because the concentration of bound species depends upon the difference between two large numbers, at least one of which is subject to error.

The *in vitro* dynamic method presented here does not purport to overcome all difficulties associated with the determination of ligand–protein interactions, but it provides certain advantages over presently available methods as well as accurately determining the degree of binding. The major advantages of this technique are:

1. It permits rapid evaluation of solute-binding characteristics.
2. Measurements can be readily performed at a series of temperatures to evaluate the enthalpy and entropy effects associated with binding interactions.
3. Simultaneous measurements of membrane permeability to various solutes are provided.
4. The technique is completely analogous to hemodialysis and permits evaluation of blood solute removal rates as well as quantifying the effect of binding interactions on dialyzer performance.

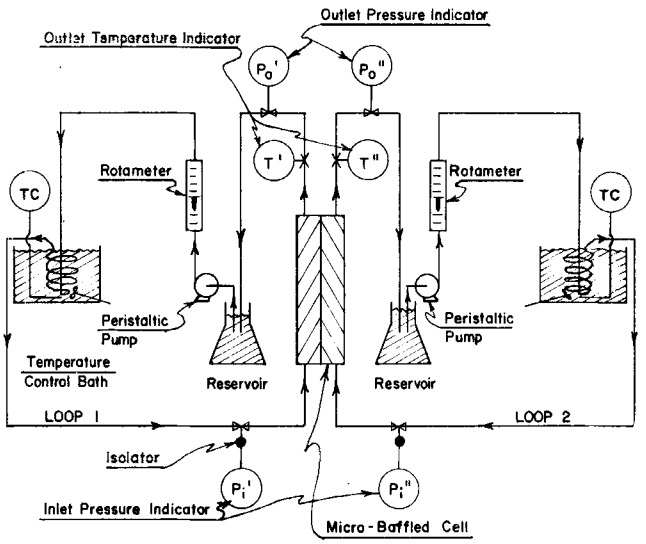

Figure 1—*Dual closed-loop dialysis system for* in vitro *binding studies.*

MATHEMATICAL MODEL

The proposed dynamic technique to determine solute–protein binding interactions is a kinetic method involving retardation of solute removal by reduction of solute activity as the result of binding. The membrane used in this study is regenerated cellulose[1], which is essentially impermeable to serum albumin and other plasma proteins (2). Consequently, any solute bound to plasma proteins becomes nondiffusable, resulting in a measurable decrease in the effective concentration driving force for molecular transfer.

A solute, exhibiting a binding affinity to proteins, exists as a free species (C_f) and a nondiffusing bound species (C_b). By assuming reversible equilibrium, the free–bound exchange can be written as:

$$\frac{\partial C_b}{\partial t} = \xi C_f - \eta C_b \qquad \text{(Eq. 1)}$$

where ξ and η are first-order association and dissociation constants.

If the membrane permeability (P_m) is the limiting resistance to mass transfer, then the membrane permeation condition is represented as:

$$\frac{dN}{dt} = -P_m A(C_{f_1} - C_{f_2}) \qquad \text{(Eq. 2)}$$

where N = mass of solute transferred, and A = effective membrane area.

If there is a significant fluid-film mass transfer resistance on either side of the membrane, then, in Eq. 2, P_m should be the overall mass transfer coefficient, h_o, defined by:

$$R\Sigma = \frac{1}{h_o} = R_m + R_{f_1} + R_{f_2} \qquad \text{(Eq. 3)}$$

[1] Cuprophan, PT 150.

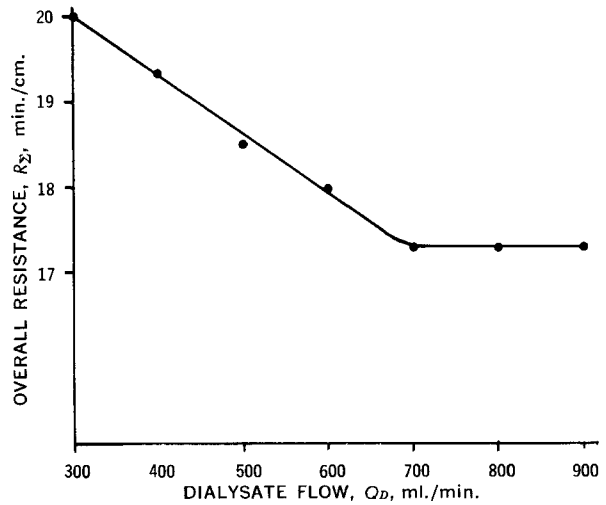

Figure 2—*Urea permeability as a function of flow rate, injection grade saline at 37°.*

where $P_m = 1/R_m$, and R_{f1} and R_{f2} are the resistances due to solute–solvent interactions on either side of the membrane.

From Eq. 1, under equilibrium conditions, $\partial C_b/\partial t$ is negligible in comparison with either term on the right-hand side. To a good approximation, $\xi C_f \simeq \eta C_b$, or:

$$\rho = \xi/\eta = C_b/C_f \qquad \text{(Eq. 4)}$$

where ρ is now referred to as the solute–protein binding coefficient.

The condition of equilibrium assumes that the time constants for binding and debinding are small compared to the smallest time constant in the system. There is a paucity of data on the kinetics of binding, but available data (3) indicate that this assumption is reasonable.

If μ refers to the plasma or human serum albumin volume fraction exclusive of proteins, it can easily be derived from Eqs. 4 and 2 that the membrane permeability can be computed for the following cases (4).

Case 1—Protein fraction in both loops 1 and 2 (Fig. 1):

$$P_m = -\frac{1}{At}\left[\frac{\mu_1\mu_2V_1V_2(1+\rho_1)(1+\rho_2)}{\mu_1V_1(1+\rho_1)+\mu_2V_2(1+\rho_2)}\right]\ln\left[\frac{C_1-\psi C_1}{C_1-\psi C_2^0}\right] \qquad \text{(Eq. 5)}$$

where $\psi = [\mu_1(1+\rho_1)]/[\mu_2(1+\rho_2)]$.

Case 2—Loop 1 contains dissolved protein (Fig. 1):

$$P_m = -\frac{1}{At}\left[\frac{\mu_1(1+\rho_1)V_1V_2}{\mu_1(1+\rho_1)V_1+V_2}\right]\ln\left[\frac{C_1-\mu_1(1+\rho_1)C_2}{C_1^0-\mu_1(1+\rho_1)C_2^0}\right] \qquad \text{(Eq. 6)}$$

Case 3—No excluded volume or protein fraction ($\mu_1 = \mu_2 = 1$ and $\rho_1 = \rho_2 = 0$):

$$P_m = -\frac{1}{At}\left(\frac{V_1 \cdot V_2}{V_1+V_2}\right)\ln\left[\frac{C_1-C_2}{C_1^0-C_2^0}\right] \qquad \text{(Eq. 7)}$$

The last equation represents the usual equation for calculating membrane solute permeability for a point dialyzer.

Equation 6 does not yield an explicit solution for the solute–protein binding coefficient ρ. Thus, the binding coefficient must be determined using an iterative technique. A digital computer program using regression analysis was written for this purpose (4). The experimental approach to determine the binding coefficient is as follows.

First, a statistically significant P_m is computed from Eq. 7 for a nonbinding environment such as saline. A separate run is then conducted from a potential solute-binding medium such as human serum albumin or plasma. Allowance is made for protein exclusion (μ_1 in Eq. 6). If the calculated P_m from Eq. 6 differs statistically from that previously obtained by Eq. 7, then binding is indicated. The correct value for ρ is then determined by increasing its value systematically from zero until (by successive iterations) the computed P_m in Eq. 6 equals the value of P_m computed from Eq. 7. When the equality is satisfied, the correct value of the binding coefficient is established. The concentrations C_1 and C_2 in Eqs. 5–7 refer to total concentrations in loops 1 and 2, respectively. Hence, in the case of Eqs. 5 and 6, C_1 and C_2 refer to the sum of free and bound solute concentrations. The other variables in the equations are well defined, with the exception of the solute–protein binding coefficient.

In using this technique, it is not mandatory that P_m be the membrane resistance solely, as long as identical experimental conditions are used for each solute in the different environments. However, an accurate assessment of solute permeability requires that fluid-film resistance be accounted for.

There are three approaches to obtain a true membrane permeability:

1. A correlation can be developed for the fluid-film mass transfer resistance so that this resistance can be subtracted from the overall resistance, as in Eq. 3.
2. A Wilson plot analogous to the heat transfer computation of Wilson (5) can be developed. This technique was used in mass transfer studies by Leonard and Bluemle (6).
3. Experiments can be run under such conditions that the turbulent boundary layer contributes negligibly to overall resistance.

The first approach depends upon developing a correlation of the form:

$$N_{SH} = aN_{Re}{}^bN_{Sc}{}^{1/3} \qquad \text{(Eq. 8)}$$

where the Sherwood and Reynolds numbers are based upon a characteristic length of the dialysate cell, such as channel height or axial length.

This approach was used very successfully by several researchers (7–10) for Leonard–Bluemle dialyzers, where the characteristic length is the membrane or cell diameter, and N_{Re} is the impeller Reynolds number. Smith *et al.* (7) characterized this type of dialyzer and developed a method whereby a true membrane permeability could be accurately determined.

The second approach is rather tedious and requires multiple runs to obtain a single permeability measurement. The third technique was used by Babb and his coworkers (11, 12); in the latter case, although the fluid-film resistance is not zero, its overall contribution can be made so low as to have a negligible effect on overall resistance, provided suitable experimental precautions are taken (4). This technique cannot be used as easily in Leonard–Bluemle dialyzers because of problems associated with membrane flutter (7), but this does not represent a serious problem for high flow in a rectangular dialyzer since transmembrane pressures are balanced and constant. This latter technique was chosen; as can be seen from Fig. 2, the overall resistance for urea transfer decreases to a minimum at a dialysate flow rate of Q_D = 700 ml./min. Figure 3 shows a similar plot for sucrose, where the overall resistance levels off at 600 ml./min. All experiments were conducted at Q_D = 800–900 ml./min. to ensure a negligible dialysate film resistance.

EXPERIMENTAL

A schematic diagram of the apparatus is shown in Fig. 1. The dialyzer used is a microbaffled unit, with a specially designed plastic innerlay containing machined baffles to induce turbulence. The average plate to membrane height is 1 mil. The present design is a modification of the B-G cell (11) and circumvents the problem of membrane puncture by nickel foam, degraded by fluid corrosion.

The apparatus consists of two separate loops with volumes of 170 ± 1 ml. Each loop contains a peristaltic pump, rotameters with needle valves to regulate pressure, temperature and pressure indicators, and a temperature-control bath able to control within ±0.05°[2].

In conducting runs, there are two possible approaches to sampling: (*a*) aliquots can be removed from the reservoir and replaced with a known concentration of solute (normally zero), or (*b*) aliquots can be taken without volume replacement such that the overall effect is negligible on the overall system volume.

[2] Equipment for use in such experiments is manufactured by Physio-Control Corp., Seattle, Wash., under license to the University of Washington.

Table I—Membrane Resistance and Permeability for Solutes Diffusing through Regenerated Cellulose[a] in Sterile, Isotonic Saline at 37°

Compound	Molecular Weight	Membrane Resistance $\pm\sigma_r$, min./cm.	Permeability, $\times 10^4$ cm./sec.
Urea[b]	60.1	16.8 ± 0.65	9.91
Guanidine	59.1	15.2 ± 0.65	10.94
Methylguanidine	73	18.3 ± 0.17	9.09
Creatinine	113.1	29.7 ± 0.53	5.62
Creatine	131.1	36.4 ± 0.39	4.58
Ur c acid[c]	168.1	36.5 ± 0.33	4.56
Lithium urate[d]	185.9	42.5 ± 0.63	3.92
Sucrose	342.3	85.5 ± 1.9	1.95
Adenosine triphosphate[e], 5.9 mg. %	507	1422.3 ± 52.9	0.12
Adenosine triphosphate, 5.9 mg. %	507	252.4 ± 5.3	0.66
Vitamin B_{12}[f]	1355	360.0 ± 5.7	0.46

[a] Cuprophan PT 150. [b] Range was 15.9–17.3 min./cm. [c] Solute concentration was 1–5 mg. %; range was 34.8–37.9 min./cm. [d] Solute concentration was 2–20 mg. %; range was 40.4–44.1 min./cm. [e] In deionized water; shows Donnan potential influence. [f] Range was 353.6–363.5 min./cm.

The first approach keeps an accurate V_1 and V_2, but there is the problem of lag time and the necessity for mass balance correction. The alternative approach results in a systematic volume error which depends upon aliquot size and number of samples. This latter approach is used. Eight to ten samples of 250 or 500 λ are taken over the course of a run. As the first and last samples do not involve volume considerations, the total volume error ranges from 0.9% to a maximum of 2.3%, with a typical error of less than 1%.

Concentration measurements are determined by liquid scintillation counting using radioactively tagged solutes (mostly ^{14}C and ^{3}H). This technique yields exceedingly accurate results. Counting efficiencies of greater than 90% for saline, human serum albumin, and plasma, and mass balance errors of better than 1.0% over 60-min. experimental runs are consistently obtainable. This assumes that there is no plating out of solute in either loop.

The scintillant cocktails are based upon the Beckman solubilizers (BBS-3 for plasma, human serum albumin, and saline; BBS-2 for blood samples), using Beckman's TLA as the fluor in reagent grade toluene. The scintillation counters used are Beckman's manual laboratory research counter (β-Mate II) and the Packard Tri-Carb Unit (model 3375). Eppendorf samplers are used for aliquot sampling at time intervals dependent upon the molecular weight of the transferring solute.

The main artifacts to be anticipated in using this technique are: (*a*) unaccounted for fluid-film mass transfer resistance, (*b*) osmotic effects, (*c*) ultrafiltration effects, (*d*) Donnan membrane potential effects, and (*e*) protein adsorption on the membrane.

The first point was already discussed. Furthermore, membrane permeability data obtained for urea, creatinine, and sucrose are in substantial agreement with published data (13).

Osmotic flow effects contribute negligibly to overall mass transfer characteristics. Estimates of the magnitude of flows indicate that its influence is insignificant (9) at physiological concentrations.

Ultrafiltration is accounted for by regulating backpressure on the exit streams of the dialysate cell. This procedure ensures that transmembrane pressures are balanced. Donnan effects, as shown by Smith *et al.* (7) and for adenosine triphosphate in this study (Table I), can be significant. However, for an isotonic saline environment, the influence of the Donnan potential is so small as to present a negligible source of error.

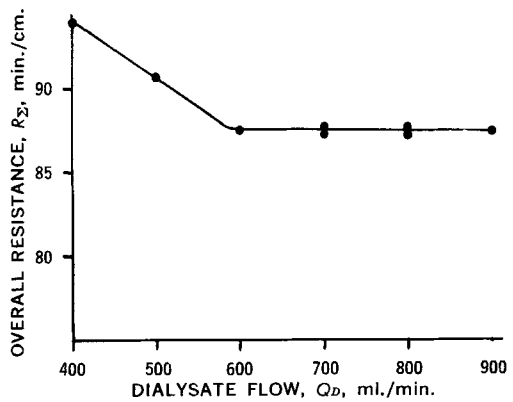

Figure 3—*Sucrose permeability as a function of flow rate, injection grade saline at 37°.*

Under normal hemodialysis conditions (laminar blood flow), it is reasonable to postulate that protein adsorption on the membrane may influence solute transfer rates. However, a recent study by Evans and Lines (14) indicated that possible thrombocytic, leucocytic, and proteinaceous deposition has a minimal effect on the blood clearance of urea and creatinine in multiple runs on a Kiil hemodialyzer. At the shear rates involved in this study, minimal interference from protein deposition would be expected. This is confirmed in this work for nonbinding solutes and in data reported by Colton *et al.* (2).

The membrane resistance shown in Tables I and II for those solutes not exhibiting binding (creatinine, creatine, vitamin B_{12}, and sucrose) are, within the limits of experimental error, the same for saline, human serum albumin, and plasma environments. Colton *et al.* (2), in studying the transport characteristics of blood-soaked cellulose membranes, reported only a 5% increase in membrane resistance for vitamin B_{12}[3] (mol. wt. = 1355) due to possible protein adsorption. These data are also within experimental error and are not significantly different from a normal saline environment.

RESULTS

Membrane permeability and resistance data for solutes of direct interest to hemodialysis studies are presented in Table I for diffusion through regenerated cellulose[1] at 37°. These data are for transfer from sterile, isotonic saline to the same solution on the other side of the membrane. With the exception of adenosine triphosphate, the membrane resistance increases approximately linearly with molecular weight, suggesting that the pore size of regenerated cellulose is considerably greater than the molecular size of vitamin B_{12}. The latter molecule closely approximates a sphere, with a diffusing area of about 223 $Å^2$ (13). In the case of adenosine triphosphate, there is a suggestion that molecular diffusion may not be occurring independently but that molecules may be associated in pairs. On the basis of molecular weight, a membrane resistance of about 130 min./cm. would be expected for adenosine triphosphate instead of the 252 min./cm. obtained. The higher resistance value for adenosine triphosphate in deionized water clearly shows the influence of the Donnan membrane potential due to the residual carboxylic groups of the cellulose.

Table II shows data on those solutes exhibiting marginal or negligible binding interactions with albumin and other plasma proteins. These data were confirmed independently by conventional ultrafiltration techniques. Table III presents data on the binding levels of two different forms of uric acid: lithium urate and virgin uric acid. The binding capacity of these two forms of uric acid differ markedly, and this fact caused considerable confusion in the

[3] Vitamin B_{12} (or one of its coenzyme forms) is known to bind reversibly at very low concentrations *in vivo* (15). This effect would be too small to be realized at 1 mg. % solute concentration.

Table II—Permeability and Resistance Data for Diffusion from Human Serum Albumin and Normal Human Plasma to Sterile, Isotonic Saline at 37° through Regenerated Cellulose[a]

Compound[b]	Medium	Apparent Membrane Resistance $\pm\sigma_r$, min./cm.	Actual Membrane Resistance $\pm\sigma_r$, min./cm.	Solute–Protein Binding Coefficient $\left(\frac{\text{g. bound/ml. plasma}}{\text{g. free/ml. plasma}}\right)$	Binding Level, %
Urea					
(100)	Human serum albumin[c] (50 g./l.)	18.0 ± 0.51	17.4 ± 0.46	0.015	1.5
(50)	Human serum albumin (50 g./l.)	15.9 ± 0.62	15.9 ± 0.62	—	—
(100)	Heparinized plasma	18.5 ± 0.40	17.3 ± 0.43	0.035	3.4
Creatinine					
(5)	Human serum albumin (50 g./l.)	30.3 ± 0.59	30.3 ± 0.59	—	—
(5)	Heparinized plasma	30.7 ± 0.73	30.7 ± 0.73	—	—
Guanidine					
(5)	Human serum albumin (50 g./l.)	22.2 ± 0.59	15.1 ± 0.65	0.195	16.3
(12)	Human serum albumin (50 g./l.)	20.1 ± 0.37	15.2 ± 0.18	0.120	10.7
Methylguanidine					
(6)	Human serum albumin (50 g./l.)	24.7 ± 0.8	18.5 ± 0.36	0.135	11.9
(6)	Heparinized plasma	26.7 ± 0.84	18.4 ± 0.25	0.225	18.4
Sucrose (20)	Human serum albumin (50 g./l.)	88.1 ± 1.53	88.1 ± 1.53	—	—
Vitamin B_{12}					
(1)	Human serum albumin (50 g./l.)	378.6 ± 5.9	378.6 ± 5.9	—	—
(1)	Citrated plasma	369.7 ± 6.4	369.7 ± 6.4	—	—
Creatine (5)	Human serum albumin (50 g./l.)	35.4 ± 0.32	35.4 ± 0.32	—	—
Adenosine triphosphate (5.9)	Human serum albumin (50 g./l.)	250.3 ± 4.9	250.3 ± 4.9	—	—

[a] Cuprophan PT 150. [b] Solute concentration (mg. %) in parentheses. [c] Albumisol (sterile, isoosmotic, pH ~7.0); Merck Sharp & Dohme.

literature (16–19). A standard technique to obtain high aqueous concentrations of the normally insoluble uric acid is to dissolve the acid with a solution of lithium carbonate at a concentration of 0.6 g./l. (20). This form of uric acid has been used in binding determinations in both plasma and human serum albumin and has resulted in considerable confusion in the reported binding levels of uric acid in normal human plasma.

From the data in Table I, it is observed that virgin uric acid has a considerably lower membrane resistance in saline solution at 37° (36.5 min./cm.) in comparison with lithium urate (42.5 min./cm.). The reduced permeability of the uricacid dissolved in lithium carbonate suggests possible chelating of lithium cations with the urate moiety. This form of complexing was observed by Albert (21) for divalent metal cations interacting with uric acid and other purines.

Table III shows that lithium urate has a considerably higher binding propensity for both human serum albumin and human plasma in comparison with virgin uric acid. For lithium urate in human serum albumin, the binding levels ranged from 20 to 40% whereas virgin uric acid had binding levels between 3 and 5%. In heparinized plasma (A + donors), the binding levels ranged from 40 to 55% whereas uric acid registered binding levels of about 5–8%. Representative data are given in Tables III and IV.

The mechanism by which the lithium urate binds is somewhat obscure, although Klotz and Loh Ming (22) established that both monovalent and divalent cations can form a bridge between protein and a normally nonbinding solute. However, this phenomenon has caused considerable confusion regarding reported binding data for uric acid to plasma proteins. Alvsaker (16–18) obtained comparable

Table III—Binding Levels and Membrane Resistance Data for Urate-Ion Diffusion through Regenerated Cellulose[a] from Human Serum Albumin and Plasma at 37°

Compound[b]	Medium	Apparent Membrane Resistance $\pm\sigma_r$, min./cm.	Actual Membrane Resistance $\pm\sigma_r$, min./cm.	Solute–Protein Binding Coefficient $\left(\frac{\text{g. bound/ml. plasma}}{\text{g. free/ml. plasma}}\right)$	Binding Level, %
Lithium urate (5)	Human serum albumin[c]	77.0 ± 1.92	42.2 ± 0.71	0.615	38.2
Lithium urate (10)	Human serum albumin	74.0 ± 1.48	42.1 ± 1.00	0.580	36.6
Lithium urate (10)	Heparinized plasma	111.2 ± 1.87	42.2 ± 0.8	1.205	55.0
Lithium urate (15)	Heparinized plasma	100.9 ± 2.00	42.1 ± 1.3	1.035	51.0
Lithium urate (10)	Citrated[d] plasma	62.9 ± 1.58	42.3 ± 1.37	0.350	26.0
Uric acid (1)	Human serum albumin	38.4 ± 0.36	36.7 ± 0.35	0.035	3.4
Uric acid (5)	Human serum albumin	39.1 ± 0.74	36.5 ± 0.41	0.050	4.8
Uric[d] acid (5)	Citrated plasma	38.6 ± 0.33	36.5 ± 0.40	0.035	3.4
Uric acid (10)	Heparinized plasma	42.0 ± 0.81	36.6 ± 0.68	0.090	8.8

[a] Cuprophan PT 150. [b] Solute concentration (mg. %) in parentheses. [c] Albumisol (50 g./l. sterile, isoosmotic); Merck Sharp & Dohme. [d] Demonstrates that citric acid interferes with urate-ion binding. This was later confirmed by ultrafiltration data (4).

Table IV—Ultrafiltration[a] Data for Solute Binding at 25°

Compound[b]	Medium	Original[c] Concentration (c.p.m.)	Filtrate Concentration	Binding Level, Percent Bound/Total
Urea (25)	Human serum albumin	57,390	58,568	1.6
Urea (25)	Heparinized plasma	65,804	67,730	3.5
Creatinine (5)	Human serum albumin	61,991	64,959	—
Creatinine (5)	Heparinized plasma	64,808	69,517	—
Lithium urate (5)	Human serum albumin	34,682	23,290	35.3
Lithium urate (5)	Heparinized plasma	34,674	18,029	51.2
Uric acid (5)	Human serum albumin	30,153	30,050	3.2
Uric acid (5)	Heparinized plasma	28,412	28,010	7.3

[a] Amicon Centri-flow membranes. [b] Solute concentration (mg. %) in parentheses. [c] Uncorrected for protein fraction volume exclusion.

binding data for both human serum albumin and plasma for uric acid predissolved in lithium carbonate, and Sheikh and Moller (19) reported the much lower binding levels obtained in this study for virgin uric acid. This issue was discussed in more detail elsewhere (23).

Table IV shows representative binding data, obtained by conventional ultrafiltration methods at 25°, which corroborate the *in vitro* closed-loop dialysis data.

The data presented here indicate that the binding levels of the major waste metabolites are small enough to be physiologically unimportant in terms of their influence on hemodialyzer performance. Also, the viability of using a dual closed-loop dialysis system to examine solute–protein binding phenomena is demonstrated. The standard deviations for those solutes exhibiting binding (Tables II and III) are comparable with equivalent data presented in Table I. Since membrane resistance data for binding solutes are obtained by an iterative procedure (4), it is encouraging that the standard deviations are so acceptable. Moreover, the fact that the dialysis technique yields binding levels equivalent to the ultrafiltration data (essentially an equilibrium method) suggests that binding equilibration for the solutes studied here is rapid. This lends support to the observations of Andreoli *et al.* (3).

Future work with this technique will center on the binding interactions of drugs and hormones that are reported to exhibit high degrees of reversible binding. For example, testosterone binding levels of 95% were reported by Hudson *et al.* (24) for normal males.

This technique not only provides estimates of the removal rates of various solutes during hemodialysis but also provides accurate determinations of solute–protein binding levels. Furthermore, because of the ease with which runs can be conducted at various temperatures, this technique can be used to calculate the variation of solute–protein binding coefficient as a function of temperature. The van't Hoff and Gibbs–Helmholtz relationships then enable enthalpy and entropy effects to be evaluated (4).

In summary, the dynamic closed-loop dialysis technique provides data of clinical importance and interest in permitting computation of: (*a*) solute removal rates for hemodialysis studies, (*b*) solute–protein binding levels, and (*c*) associated thermodynamic properties. This technique could prove useful as a clinical and research adjunct for both pharmacological and endocrinological investigations.

REFERENCES

(1) J. Steinhardt and J. A. Reynolds, "Multiple Equilibria in Proteins," Academic, New York, N. Y., and London, England, 1969.

(2) C. K. Colton, K. A. Smith, E. W. Merrill, and P. C. Farrell, to be published.

(3) K. Andreoli, J. Robbins, J. E. Hall, and M. Bermore, *Proc. Int. Thyroid Conf., 5th*, **1965**, 635; *Reference 1*, p. 341.

(4) P. C. Farrell, Ph.D. thesis, University of Washington, Seattle, Wash., 1971.

(5) E. E. Wilson, *Trans. Amer. Soc. Mech. Eng.*, **37**, 47(1915).

(6) E. F. Leonard and L. W. Bluemle, Jr., *Trans. Amer. Soc. Artif. Intern. Organs*, **8**, 182(1962).

(7) K. A. Smith, C. K. Colton, E. W. Merrill, and L. B. Evans, *Chem. Eng. Prog. Symp. Ser.*, **64**, 45(1968).

(8) T. C. Kaufman and E. F. Leonard, *A.I.Ch.E.J.*, **14**, 110 (1968).

(9) P. C. Farrell, M. S. thesis, Massachusetts Institute of Technology, Cambridge, Mass., 1967.

(10) L. J. Friedman, M. S. thesis, Columbia University, New York, N. Y., 1966.

(11) L. Grimsrud and A. L. Babb, *Chem. Eng. Prog. Symp. Ser.*, **62**, 19(1966).

(12) A. L. Babb, C. J. Maurer, D. L. Fry, R. P. Popovich, and R. E. McKee, *ibid.*, **64**, 59(1968).

(13) C. K. Colton, Ph.D. thesis, Massachusetts Institute of Technology, Cambridge, Mass., 1969.

(14) D. B. Evans and J. G. Lines, *Brit. Med. J.*, **1**, 786(1970).

(15) C. A. Hall and A. E. Finkler, *Biochim. Biophys. Acta*, **78**, 234(1963).

(16) J. O. Alvsaker, *Scand. J. Clin. Lab. Invest.*, **17**, 467(1965).

(17) *Ibid.*, **17**, 476(1965).

(18) *Ibid.*, **18**, 227(1966).

(19) M. J. Sheikh and J. V. Moller, *Biochim. Biophys. Acta*, **158**, 456(1968).

(20) E. Praetorius, "Uricase-Studier," Rosenkilde and Bagger, Copenhagen, Denmark, 1949.

(21) A. Albert, *Biochem. J.*, **54**, 646(1953).

(22) I. M. Klotz and W. C. Loh Ming, *J. Amer. Chem. Soc.*, **76**, 805(1954).

(23) P. C. Farrell, R. P. Popovich, and A. L. Babb, *Biochim. Biophys. Acta*, **229**, 222(1971).

(24) B. Hudson, H. G. Burger, D. M. de Kretser, J. P. Coghlan, and H. P. Taft, in "The Human Testis," E. Rosenberg and C. A. Paulsen, Eds., Plenum, New York, N. Y., and London, England, 1970.

ACKNOWLEDGMENTS AND ADDRESSES

Received March 11, 1971, from the *Departments of Chemical and Nuclear Engineering, University of Washington, Seattle, WA 98105*

Accepted for publication June 2, 1971.

This study was supported by Contract PH 43-66-932 from the National Institute of Arthritic and Metabolic Diseases, National Institutes of Health, Public Health Service, U.S. Department of Health, Education, and Welfare.